



***In silico* Study of Transmural Dispersion of Repolarization in Non-failing Human Ventricular Myocytes: Contribution to Cardiac Safety Pharmacology**

Bernard Christophe^{1*}

¹SCAP Test, rue d'Albroux 10, B-1367 Grand Rosière Hottomont, Belgium.

Author's contribution

The sole author designed, analyzed and interpreted and prepared the manuscript.

Article Information

DOI: 10.9734/BJPR/2015/17850

Editor(s):

(1) Alyautdin Renad N, Chair of The Department of Pharmacology (Pharmaceutical Faculty), I. M. Sechenov MSMU, Moscow, Russia.

Reviewers:

- (1) Pietro Scicchitano, Cardiology Department, Hospital "F. Perinei" Altamura (Bari), Italy.
(2) Alexander Berezin, Internal Medicine Department, Zaporozhye Medical University, Ukraine.
(3) Emre Yalcinkaya, Department of Cardiology, Malatya Military Hospital, Malatya, Turkey.
(4) A. Papazafropoulou, Department of Internal Medicine and Diabetes Center, Tzaneio General Hospital of Piraeus, Greece.
(5) William T. Clusin, Department of Medicine (Cardiology), Stanford University School of Medicine, USA.
Complete Peer review History: <http://www.sciencedomain.org/review-history.php?iid=1177&id=14&aid=9467>

Original Research Article

Received 27th March 2015
Accepted 7th May 2015
Published 28th May 2015

ABSTRACT

Aims: To investigate the putative usefulness of the *in silico* determination of transmural dispersion of repolarization (TDR) for early cardiac safety pharmacology.

Study Design: Computational simulations.

Place and Duration of Study: SCAP Test, Belgium, between September 2014 and March 2015.

Methodology: TDR was calculated as the difference between epicardial-midmyocardial action potential duration (APD₉₅) determined in non-failing human ventricular myocytes using the O'Hara-Rudy dynamic algorithm. The role of each ionic current in TDR was investigated by modifying its conductance in the algorithm. The effects of each tested drug on TDR were studied by reducing the I_{Kr}, I_{Na} and I_{CaL} conductances in the algorithm by a scaling factor which is a function of the IC₅₀ of the drug for I_{Kr}, I_{Na} and I_{CaL} ionic currents and the maximal effective free therapeutic plasma concentration (EFTPC_{max}) of the drug.

Results: Our simulations showed that TDR was increased by a preferential midmyocardial APD₉₅ prolongation which was induced by net repolarising current reduction via I_{Kr} or I_{Ks} inhibition and/or

*Corresponding author: Email: bchristophe@scaptest.com;

I_{CaL} or I_{NaL} activation. Drugs' effects on TDR were in good agreement with their torsade de pointes (TdP) risk according to the CredibleMeds or the Redfern classifications: most torsadogenic tested drugs induced a TDR increase via I_{Kr} vs. I_{CaL} and/or I_{Na} selective inhibition; while most non-torsadogenic tested drugs induced a TDR decrease via I_{CaL} vs. I_{Kr} and/or I_{Na} selective inhibition.
Conclusion: Based on computer simulations within the human situation, the present study identified the effects of various cardiac ionic currents on TDR amplitude and suggested that *in silico* study of drugs' effects on TDR could be informative for early cardiac safety pharmacology.

Keywords: Transmural dispersion of repolarization; safety pharmacology; *in silico* cardiac action potential simulation; human ventricular myocytes; I_{Kr} , I_{Na} and I_{CaL} cardiac ionic currents; early afterdepolarization; maximal effective free therapeutic plasma concentration.

ABBREVIATIONS

AP: action potential, APA: AP amplitude, APD_{xx} : AP duration at xx percent of its amplitude, EAD: early after depolarization, $EFTPC_{max}$: maximal effective free therapeutic plasma concentration, ORd: O'Hara-Rudy dynamic algorithm, TdP: torsade de pointes, TDR: transmural dispersion of repolarization, V_{max} : maximal rate of AP rise.

1. INTRODUCTION

Prediction of an unacceptable risk of torsade de pointes (TdP) remains a major goal of cardiac safety pharmacology. In order to detect drug candidate cardiac liabilities, the current non-clinical guidance for safety pharmacology studies is based on the detection of (i) cardiac I_{Kr} current inhibition by *in vitro* human ether-à-go-go-related gene (hERG) electrophysiological assay, (ii) abnormal action potential (AP) time course using isolated cardiac tissues, and (iii) the difference between Q and T waves (QT interval) on the electrocardiogram using an *in vivo* model [1]. Nevertheless, as the corrected QT interval prolongation has been afterwards proven to be a poor specific marker of TdP occurrence within the human situation, some drug candidates have been accurately or unreasonably rejected [2,3]. Moreover, other cardiac ionic currents different from hERG current also influence the AP time course so that a multiple ionic channels block approach is recognized as important for the improvement of the early prediction of clinical torsadogenic risk of drugs [4,5]. Therefore, a new approach, the comprehensive *In vitro* pro-arrhythmia assay (CiPA) initiative [2,3], is currently under evaluation [6,7]. The detection of drug candidate cardiac liabilities with the CiPA initiative is based on (i) The measurement of functional effects on multiple cardiac currents measured by voltage clamp technology, (ii) The prediction of effects on AP by *in silico* simulations, and (iii) The confirmation of effects on AP by integrated human cellular electrophysiological studies. During the last decade, the utility of computational simulations

has become increasingly accepted [8-12]. Indeed, multiple loops occurring between experimental results and modelling have progressively increased the refinement of these computer algorithms and thus the confidence that can be placed in them. These simulations can be carried out faster, cheaper and earlier during the drug candidate discovery research early process directly within the human situation, without use of animal testing. Using these computational simulations, various parameters (such as action potential duration (APD), triangulation, early afterdepolarization (EAD), transmural dispersion of repolarization (TDR), reverse use dependence (RUD),...) could be studied in detail under various experimental conditions (such as variations in cycle length, different ionic compositions, cardiac channels activation/inhibition,...). The aim of the present work was to study the usefulness of *in silico* TDR determination for early cardiac safety pharmacology. Indeed, a higher APD increase in the midmyocardial vs. epicardial myocytes induces TDR increase, providing a substrate for TdP [13]. The APs observed from *in silico* simulations with the O'Hara-Rudy dynamic (ORd) algorithm were similar to the APs measured on the coronary perfused isolated human left ventricular wedge preparation [14,15]. Moreover, this ORd algorithm takes into account the ventricular transmural heterogeneity showing a longer APD in midmyocardial vs. epi- and endocardial myocytes, as first identified by Antzelevitch et al. [16]. In consequence, the present study was performed using *in silico* simulations with this ORd algorithm in an attempt to calculate TDR, to determine its cardiac current

dependence and also to evaluate the effects of various drugs on this TDR amplitude.

2. MATERIALS AND METHODS

The ORd algorithm was fully described by O'Hara et al. [14] and in the research section of their website (<http://rudylab.wustl.edu>). Equations, constants (extracellular ionic concentrations, cell geometry, channel conductance), initial conditions for state variables and scaling factors (applied to various ionic fluxes or to the conductance of various channels allowing the testing of differences among endo-, mid- and epimyocardial cells) were used as described in the ORd algorithm. Simulations were carried out at equilibrium (after 100 beats). The difference between APD₉₅ (chosen in order to maximize the difference between various types of myocytes) calculated for midmyocardial and epicardial myocytes was used in order to estimate TDR without taking into account the propagation of the stimulation across the ventricular wall (estimated to 22 ms in the arterially perfused isolated dog ventricular wedge preparation, for example [17]). The effect of activation or inhibition of I_{Kr}, I_{Ks}, I_{Na}, I_{to}, I_{NaL} or I_{CaL} currents on TDR was tested by shifting the conductance of these channels as described by Mirams et al. [4]. The testing of the effects of compounds was based on the data set published by Kramer et al. [5] describing the 50% inhibitory concentration values (IC_{50s}) and hill coefficients for hERG, hCav1.2 and hNav1.5 currents (measured by QPatch and PatchXpress automatic patch system) and the maximal effective free therapeutic plasma concentration (EFTPC_{max}) of fifty-five compounds (categorized by Kramer et al. [5] as torsadogenic (thirty-two compounds) or non-torsadogenic (twenty-three compounds)). The great advantage of this data set was the large number of compounds studied using human genes for the determination of their effects on various cardiac channels and the well balanced distribution of these compounds with regard to their TdP risk classification. According to Redfern et al. [18], compounds can be categorized into five classes: Class I (class Ia or III anti-arrhythmics having a large but acceptable TdP risk), class II (compounds withdrawn from the market due to unacceptable TdP risk), class III (compounds with numerous TdP reports), class IV (compounds with isolated TdP reports) and class V (compounds without any published TdP reports). According to CredibleMeds [19], compounds can be categorized into three classes: class 1 (compounds that are generally

accepted by the QT drugs.org advisory Board to carry a risk of TdP), class 2 (compounds with possible risk of TdP) and class 3 (compounds with conditional risk of TdP). The effects of the tested compounds on TDR were studied by reducing the I_{Kr}, I_{Na} and I_{CaL} conductances in the ORd algorithm by a scaling factor which is a function of the IC₅₀ of the compounds for I_{Kr}, I_{Na} and I_{CaL} ionic currents and a multiple (1-fold, 3-fold, 10-fold, 30-fold or 100-fold) of the EFTPC_{max} of the compounds, as described by Mirams et al. [4].

3. RESULTS AND DISCUSSION

3.1 TDR Determination

The importance of TDR in cardiac safety pharmacology is now fully recognized, as a TDR increase provides a substrate for EAD and TdP as already extensively reported and discussed in the literature [13,20-22]. Conversely, a TDR decrease leads to TdP prevention, as observed with mexiletine [23] or pentobarbital [22]. Using the ORd algorithm under a cycle length (CL) of 1000 ms at equilibrium, stimulation of isolated non-failing human ventricular epicardial, midmyocardial or endocardial myocytes (Fig. 1) induced an AP characterized by similar amplitude but different shapes. A peak and dome shape was observed on epicardial and midmyocardial myocytes while no peak and dome shape was observed on endocardial myocytes. Under these simulation conditions, the APD₉₅ amplitude was calculated to be 239, 278 and 356 milliseconds (ms) for epicardial, endocardial and midmyocardial myocytes, respectively. Under these experimental conditions, the reference TDR was calculated to be 117 ms.

This TDR amplitude was inversely proportional to the cycle length (Fig. 2). Based on this result, a cycle length of 1000 ms, which is near to basal heart rate conditions, was chosen for the study of the effects of ionic currents and drugs on TDR.

3.2 Effect of Ionic Currents on TDR

Gradual inhibition of I_{Kr} current (Fig. 3) induced a gradual TDR increase until an I_{Kr} inhibition of 68% was reached. At this level of I_{Kr} inhibition, TDR was calculated to be 249 ms. This TDR increase was linked to a higher APD₉₅ increase in the midmyocardial vs. epi- or endocardial myocytes (APD₉₅ increase of 86, 72 and 70%, respectively). Above this 68% I_{Kr} inhibition, EAD was observed on the midmyocardial myocytes.

By contrast, a full inhibition of I_{Ks} or I_{to} (Fig. 3) induced a lower TDR increase to a value of 140 or 122 ms, respectively. Conversely, a full inhibition of I_{CaL} current (Fig. 3) decreased TDR to a value of 90 ms. An I_{Na} inhibition of 85% (Fig. 3) induced a lower TDR decrease to a value of 114 ms. Above this inhibition level, decrease in maximal AP amplitude (APA) (69 vs. 129 mV under control conditions) and in maximal rate of rise (V_{max}) (80 vs. 245 V/s under control conditions) was measured on the midmyocardial myocytes. A full inhibition of I_{NaL} also induced a TDR decrease to a value of 105 ms.

A 3-fold activation of I_{Kr} , I_{Ks} or I_{to} (data not shown) induced a TDR decrease to a value of 74, 93 or 100 ms, respectively. A 3-fold activation of I_{NaL} or I_{CaL} (data not shown) induced a TDR increase to a value of 138 or 158 ms, respectively. A 3-fold activation of I_{Na} (data not shown) induced a TDR increase to a value of 119 ms.

Taken together, these data fully confirmed the ionic current dependence of TDR experimentally observed in the most frequently used model: the isolated dog left ventricular preparation. In this preparation, TDR was shown to be increased by a preferential midmyocardial prolongation of APD by compounds that reduce net repolarizing current via I_{Kr} or I_{Ks} inhibition or I_{CaL} or I_{NaL} activation [21,22,24]. In consequence, *in silico* simulation can be used to determine if a compound induces a TDR increase or decrease

due to its inhibiting and/or activating effects on the various cardiac ionic currents. Moreover, this methodology can also detect if this TDR increase leads to EAD formation.

3.3 Effect of Drugs on TDR

We studied the effects on TDR amplitude of 55 compounds reported by Kramer and al. [5] as torsadogenic (32 compounds, Fig. 4A) or non-torsadogenic (23 compounds, Fig. 4B).

Based on our *in silico* simulations, seven profiles of compounds (Fig. 4) were identified: compounds inducing a gradual TDR increase providing a substrate for EAD (profile 1), compounds inducing a gradual TDR increase without any EAD (profile 2), compounds inducing a partially reversible TDR increase (profile 3), compounds with no effect on TDR (profile 4), compounds inducing a TDR decrease (profile 5), compounds inducing a partially reversible TDR decrease (profile 6), and finally compounds inducing a TDR decrease associated to APA and V_{max} decreases (profile 7). In order to determine if these seven profiles could be related to the compounds properties, the various ratios of I_{Kr} , I_{Na} or I_{CaL} IC_{50s} to $EFTPC_{max}$ reported for each compound by Kramer et al. [5] were illustrated by Fig. 5 (profiles 1 and 2) and Fig. 6 (profiles 3 to 7).

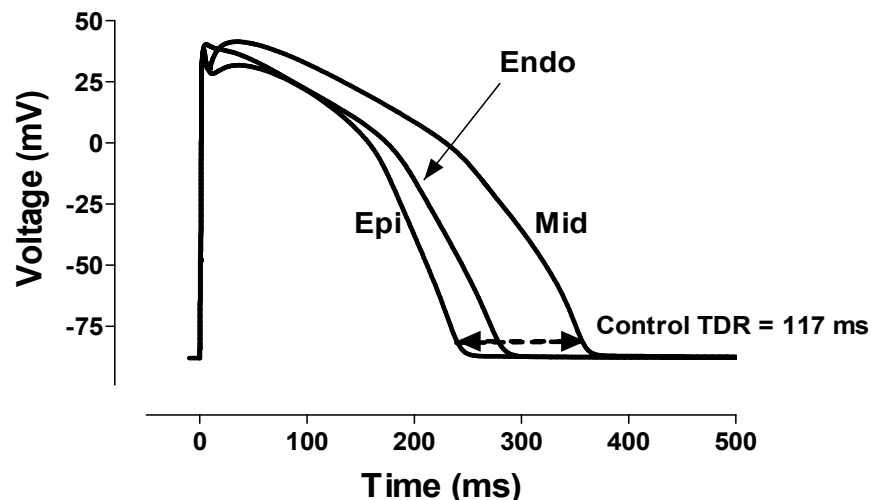


Fig. 1. AP time course determined by *in silico* simulation using the ORd algorithm in non-failing human ventricular epicardial (Epi), midmyocardial (Mid) and endocardial (Endo) myocytes under a cycle length of 1000 ms at equilibrium

The dotted line represents TDR calculated as the difference between APD_{95mid} and APD_{95epi} . The abscissa is the time expressed as milliseconds (ms). The ordinate is the membrane voltage expressed as millivolts (mV)

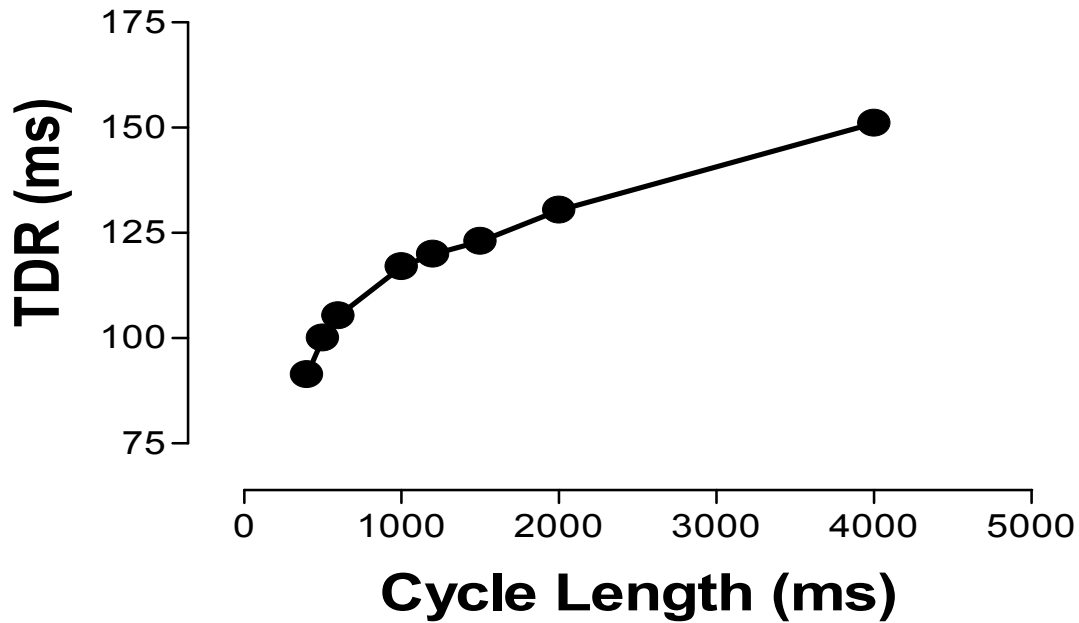


Fig. 2. Effect of the cycle length on the TDR amplitude
 The abscissa is the cycle length duration expressed as milliseconds (ms). The ordinate is the TDR expressed as milliseconds (ms)

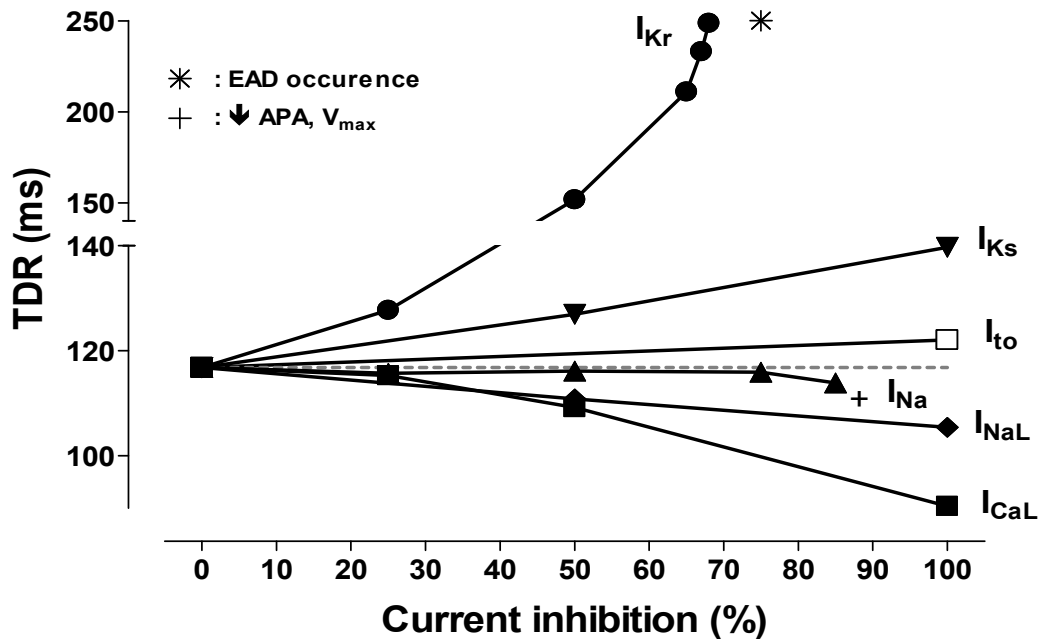


Fig. 3. Effect of various ionic currents inhibition on the TDR amplitude
 The ●, ▼, □, ▲, ◆ and ■ symbols represent the TDR amplitude observed after I_{Kr} , I_{Ks} , I_{to} , I_{NaL} , I_{NaL} or I_{CaL} inhibition, respectively. The dotted line represents the control value (117 ms). The * symbol represents EAD occurrence at I_{Kr} inhibition higher than 68 %. The + symbol represents APA and V_{max} decreases at I_{Na} inhibition higher than 85 %. The abscissa is the amplitude of the ionic current inhibition expressed as percent (%). The ordinate is the TDR amplitude expressed as milliseconds (ms)

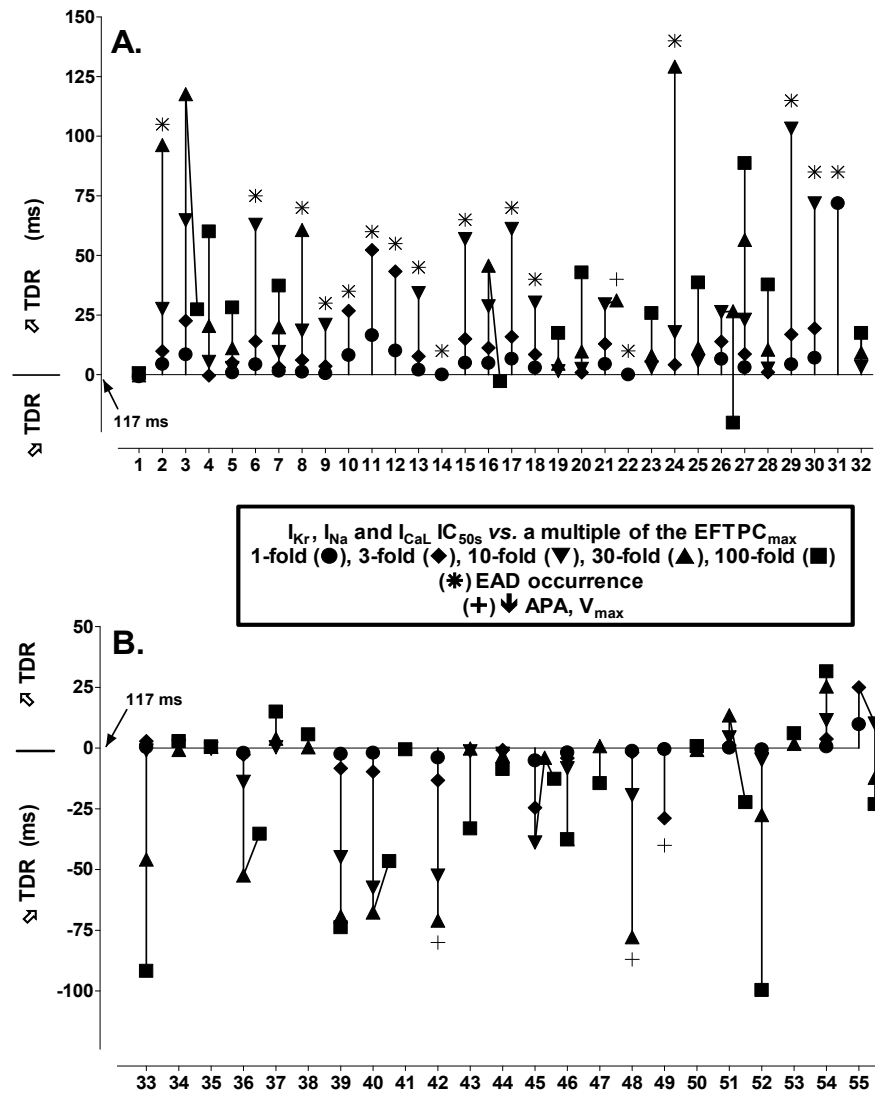


Fig. 4. Effects of various compounds on TDR amplitude

Effects on TDR amplitude of 32 torsadogenic (A) and 23 non-torsadogenic (B) compounds (as reported by Kramer et al. [5]). The effects of the tested compounds on TDR were studied by reducing the I_{Kr} , I_{Na} and I_{CaL} conductances by a scaling factor which is a function of the IC_{50s} of the compounds for I_{Kr} , I_{Na} and I_{CaL} ionic currents and a multiple (1-fold (●), 3-fold (◆), 10-fold (▼), 30-fold (▲) and 100-fold (■)) of $EFTPC_{max}$ of the compounds [4]. The * symbol represents an EAD occurrence at the step just above the last represented symbol. The + symbol represents APA and V_{max} decreases at the step just above the last represented symbol. The abscissa is the reference number of each compound numbered as follows: (1) amiodarone, (2) astemizole, (3) bepridil, (4) chlorpromazine, (5) cilostazol, (6) cisapride, (7) clozapine, (8) disopyramide, (9) dofetilide, (10) droperidol, (11) flecainide, (12) halofantrine, (13) haloperidol, (14) ibutilide, (15) methadone, (16) moxifloxacin, (17) nilotinib, (18) paliperidone, (19) paroxetine, (20) pimozide, (21) procainamide, (22) quinidine, (23) risperidone, (24) sertindole, (25) solifenacin, (26) sotalol, (27) sparfloxacin, (28) sunitinib, (29) terfenadine, (30) terodiline, (31) thioridazine, (32) voriconazol, (33) ceftriaxone, (34) dasatinib, (35) diazepam, (36) diltiazem, (37) donepezil, (38) duloxetine, (39) lamivudine, (40) linezolid, (41) loratadine, (42) metronidazole, (43) mibefradil, (44) mitoxantrone, (45) nifedipine, (46) nitrendipine, (47) pentobarbital, (48) phenytoin, (49) piperacillin, (50) raltegravir, (51) ribavirin, (52) saquinavir, (53) sitagliptin, (54) telbivudine and (55) verapamil. The ordinate is the TDR increase (Δ TDR) or decrease (Δ TDR) expressed as milliseconds (ms). The zero ordinate value represents control TDR (117 ms) in the absence of any compound

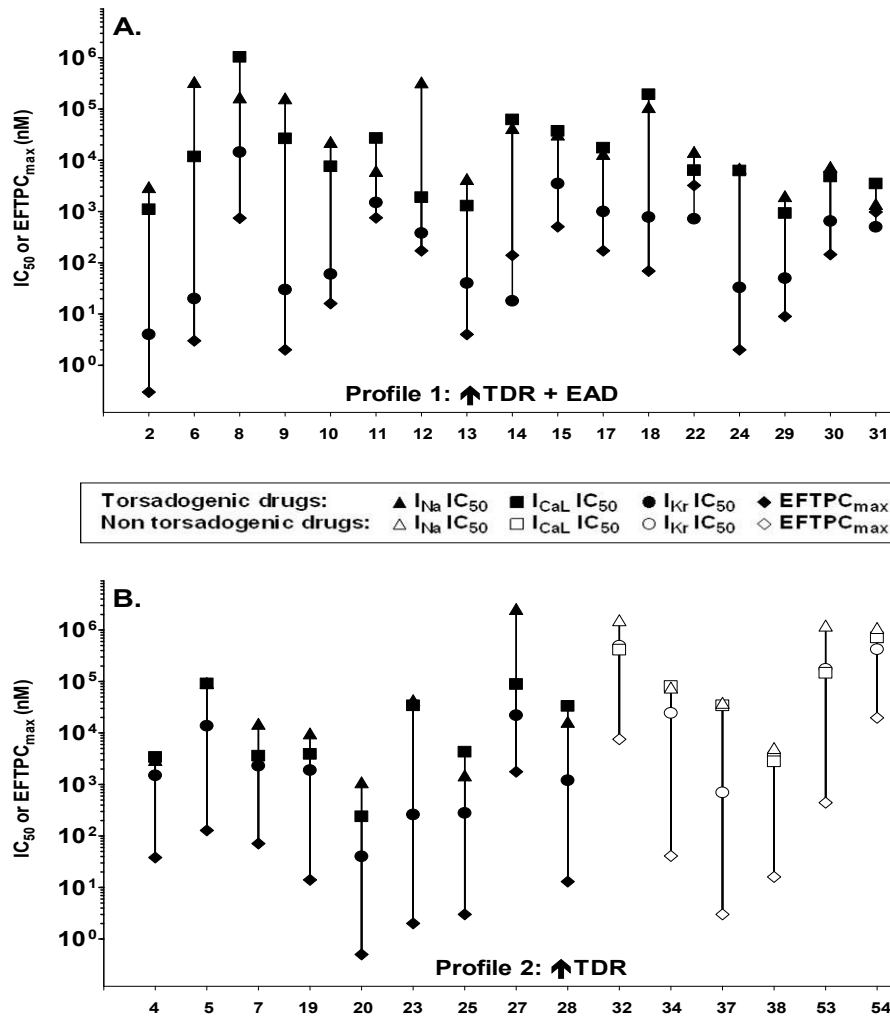


Fig. 5. EFTPC_{max} and IC₅₀ values for I_{Kr}, I_{Na} or I_{CaL} of compounds identified as belonging to profile 1 (A) or profile 2 (B) with regard to their activity on TDR

EFTPC_{max} (◆ or ◇) and IC₅₀ values for I_{Kr} (● or ○), I_{Na} (▲ or △) or I_{CaL} (■ or □) of torsadogenic (closed symbols) and non-torsadogenic (open symbols) compounds (as calculated or reported by Kramer et al. [5]). The ◆-● or ◇-○ lines represent the logarithm of the ratio of I_{Kr} inhibition to EFTPC_{max}. The ◆-■ or ◇-□ lines represent the logarithm of the ratio of I_{CaL} inhibition to EFTPC_{max}. The ◆-▲ or ◇-△ lines represent the logarithm of the ratio of I_{Na} inhibition to EFTPC_{max}. The abscissa is the reference number of each compound numbered as shown in Fig. 4. The ordinate is the IC₅₀s or the EFTPC_{max} expressed as nanomolar (nM) on a logarithmic scale

Seventeen compounds (Fig. 4A) were identified as belonging to profile 1. They first induced a gradual TDR increase, followed by EAD occurrence at 100-fold (astemizole, disopyramide and sertindole), 30-fold (cisapride, dofetilide, haloperidol, methadone, nilotinib, paliperidone, terfenadine and terodiline), 10-fold (droperidol, flecainide and halofantrine), 3-fold (thioridazine) or 1-fold (ibutilide and quinidine) their EFTPC_{max}. These compounds (Fig. 5A) showed an I_{Kr} IC₅₀ / EFTPC_{max} ratio ranked from 0.1-fold to 19.4-fold,

an I_{Kr} vs. I_{CaL} selectivity ranked from 5-fold to 3472-fold and an I_{Kr} vs. I_{Na} selectivity ranked from 3-fold to 16850-fold. These seventeen compounds (Fig. 7) were reported as torsadogenic by Kramer et al. [5]. When they are categorized according to their TdP risk, these compounds were categorized as belonging to classes I, II or III of the Redfern classification [18] or to classes 1 or 2 of the CredibleMeds classification [19].

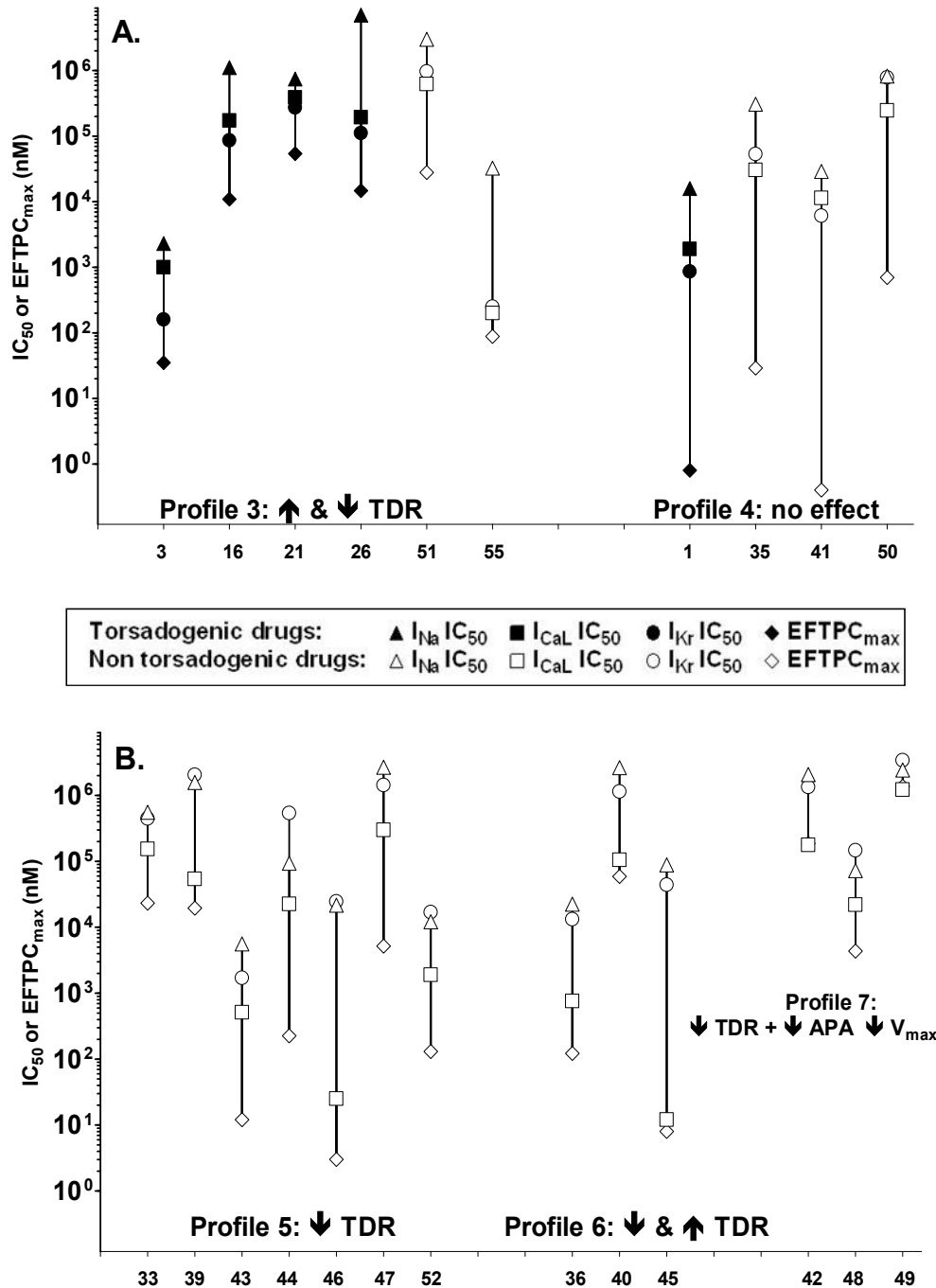


Fig. 6. EFTPC_{max} and IC₅₀ values for I_{Kr}, I_{Na} or I_{CaL} of compounds identified as belonging to profiles 3 and 4 (A) or profiles 5, 6 and 7 (B) with regard to their activity on TDR
EFTPC_{max} (◆ or ◇) and *IC₅₀* values for *I_{Kr}* (● or ○), *I_{Na}* (▲ or △) or *I_{CaL}* (■ or □) of torsadogenic (closed symbols) and non-torsadogenic (open symbols) compounds (as calculated or reported by Kramer et al. [5]). The ◆-● or ◇-○ lines represent the logarithm of the ratio of *I_{Kr}* inhibition to *EFTPC_{max}*. The ◆-■ or ◇-□ lines represent the logarithm of the ratio of *I_{CaL}* inhibition to *EFTPC_{max}*. The ◆-▲ or ◇-△ lines represent the logarithm of the ratio of *I_{Na}* inhibition to *EFTPC_{max}*. The abscissa is the reference number of each compound numbered as shown in Fig. 4. The ordinate is the *IC₅₀*s or the *EFTPC_{max}* expressed as nanomolar (nM) on a logarithmic scale

Fifteen compounds (on the one hand (Fig. 4A) chlorpromazine, cilostazol, clozapine, paroxetine, pimozide, risperidone, solifenacin, sparfloracin, sunitinib and voriconazole and on the other (Fig. 4B) dasatinib, donepezil, duloxetine, sitagliptin and telbivudine) were identified as belonging to profile 2. These compounds induced a gradual TDR increase without any EAD up to 100-fold their $EFTPC_{max}$ (maximal TDR increase of 89 ms for sparfloracin, for example). These compounds (Fig. 5B) showed an $I_{Kr} IC_{50} / EFTPC_{max}$ ratio ranked from 13-fold to 598-fold, an I_{Kr} vs. I_{CaL} selectivity ranked from 0.8-fold to 132-fold and an I_{Kr} vs. I_{Na} selectivity ranked from 1.3-fold to 167-fold. These fifteen compounds (Fig.7) were reported as torsadogenic or non-torsadogenic by Kramer et al. [5]. When they are categorized according to their TdP risk, these compounds were categorized as belonging to classes III, IV or V of the Redfern classification [18] or to classes 1, 2 or 3 of the CredibleMeds classification [19].

Six compounds (on the one hand (Fig. 4A) bepridil, moxifloxacin, procainamide and sotalol and on the other (Fig. 4B) ribavirin and verapamil) were identified as belonging to profile 3. Bepridil (Fig. 4A) induced first a gradual TDR increase (maximum of 118 ms) up to 30-fold its $EFTPC_{max}$ followed by a lower TDR increase (27 ms) at 100-fold its $EFTPC_{max}$. Moxifloxacin and sotalol (Fig. 4A) and ribavirin (Fig. 4B) induced first a gradual TDR increase (maximum of 46, 27, and 13 ms for moxifloxacin, sotalol, and ribavirin, respectively) up to 30-fold their $EFTPC_{max}$ followed by a TDR decrease (-3, -22 and -22 ms for moxifloxacin, sotalol and ribavirin, respectively) at 100-fold their $EFTPC_{max}$. Verapamil (Fig. 4B) induced first a gradual TDR increase (maximum of 25 ms) up to 3-fold its $EFTPC_{max}$ followed by a TDR decrease (-23 ms) at 100-fold their $EFTPC_{max}$. Procainamide (Fig. 4A) induced a gradual TDR increase up to 30-fold its $EFTPC_{max}$ (maximum of 31.1 ms). At 30-fold its $EFTPC_{max}$, a decrease in AP amplitude (97 vs. 129 mV without compound) and in V_{max} (80 vs. 245 V/s without compound) was observed in the midmyocardial myocytes. These six compounds (Fig. 6A) showed an $I_{Kr} IC_{50} / EFTPC_{max}$ ratio ranked from 3-fold to 35-fold, an I_{Kr} vs. I_{CaL} selectivity ranked from 0.6-fold to 6-fold and an I_{Kr} vs. I_{Na} selectivity ranked from 3-fold to 130-fold. These six compounds (Fig. 7) were reported as torsadogenic or non-

torsadogenic by Kramer et al. [5]. When they are categorized according to their TdP risk, bepridil, moxifloxacin, procainamide and sotalol were categorized as belonging to classes I or III of the Redfern classification [18] or to class 1 of the CredibleMeds classification [19] when verapamil was categorized as belonging to class V of the Redfern classification [18].

Four compounds (on the one hand (Fig. 4A) amiodarone and on the other (Fig. 4B) diazepam, loratadine and raltegravir) were identified as belonging to profile 4. These compounds did not induce any TDR change even at 100-fold their $EFTPC_{max}$. These four compounds (Fig. 6A) showed an $I_{Kr} IC_{50} / EFTPC_{max}$ ratio ranked from 1075-fold to 15250-fold and an I_{Kr} vs. I_{Na} selectivity ranked from 1-fold to 8-fold. Amiodarone and loratadine showed an I_{Kr} vs. I_{CaL} selectivity of 2-fold while diazepam and raltegravir showed an I_{CaL} vs. I_{Kr} selectivity of 2-fold to 3-fold, respectively. These four compounds (Fig. 7) were reported as torsadogenic or non-torsadogenic by Kramer et al. [5]. When they are categorized according to their TdP risk, amiodarone was categorized as belonging to class I of the Redfern classification [18] or to class 1 of the CredibleMeds classification [19] while loratadine was categorized as belonging to class V of the Redfern classification [18].

Seven compounds (ceftriaxone, lamivudine, mibefradil, mitoxantrone, nitrendipine, pentobarbital and saquinavir) were identified as belonging to profile 5. These compounds (Fig. 4B) induced a gradual TDR decrease up to 100-fold their $EFTPC_{max}$ (maximal decrease of -100 ms for saquinavir, for example). These compounds (Fig. 6B) showed an $I_{Kr} IC_{50} / EFTPC_{max}$ ratio ranked from 19-fold to 8200-fold. In contrast to compounds belonging to profiles 1 to 4, these seven compounds (Fig. 6B) showed an $I_{CaL} IC_{50}$ lower than their $I_{Kr} IC_{50}$. They showed an I_{CaL} vs. I_{Kr} selectivity ranked from 4-fold to 864-fold and an I_{CaL} vs. I_{Na} selectivity ranked from 3-fold to 984-fold. These seven compounds (Fig. 7) were reported as non-torsadogenic by Kramer et al. [5]. When they are categorized according to their TdP risk, mibefradil and nitrendipine were categorized as belonging to classes IV or V of the Redfern classification [18], respectively.

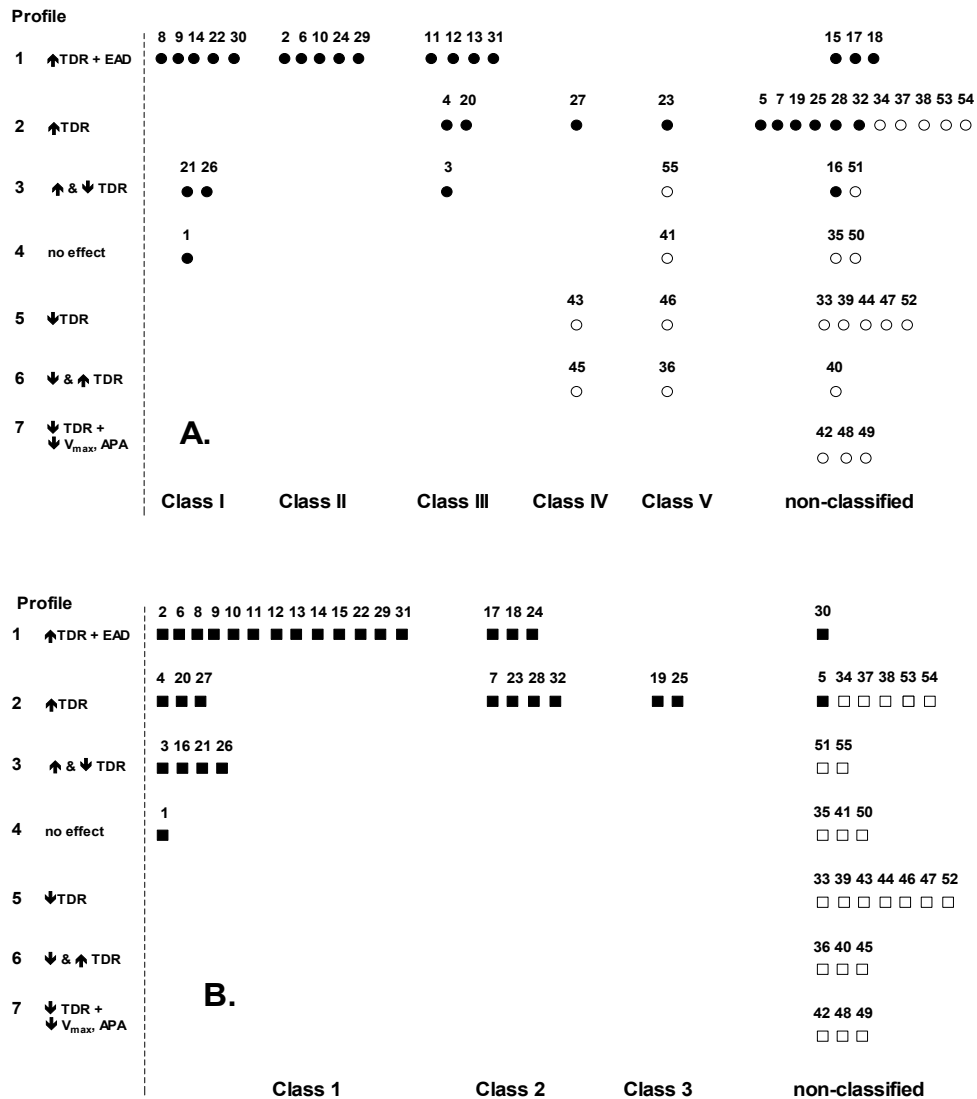


Fig. 7. Distribution of the various tested compounds through their activity profile on TDR and their TdP risk according to the classification of Redfern et al. (A) or the CredibleMeds (B) classification

Thirty-two torsadogenic (closed symbols) and twenty-three non-torsadogenic (open symbols) tested compounds (as reported by Kramer et al. [5]) were distributed through their activity profile on TDR and their TdP risk classification according to (A) the classification of Redfern et al. (● or ○) [18] or to (B) the CredibleMeds classification (■ or □) [19]. The two TdP risk classifications are described in the methods section. Non-classified compounds are compounds not reported in the Redfern or CredibleMeds classifications. Tested compounds are numbered as shown in Fig. 4

Three compounds (diltiazem, linezolid and nifedipine) were identified as belonging to profile 6. These compounds (Fig. 4B) induced first a gradual TDR decrease up to 10 to 30-fold their EFTPC_{max} (maximum -68 ms for linezolid, for example) followed by a lower TDR decrease at 30 to 100-fold their EFTPC_{max} (-46 ms for linezolid, for example). These compounds

showed (Fig. 6B) an I_{Kr} IC₅₀ / EFTPC_{max} ratio ranked from 19-fold to 5500-fold. As compounds from profile 5, these compounds (Fig. 6B) showed an I_{CaL} IC₅₀ lower than their I_{Kr} IC₅₀. They showed an I_{CaL} vs. I_{Kr} selectivity ranked from 25-fold to 7375-fold and an I_{CaL} vs. I_{Na} selectivity ranked from 11-fold to 3667-fold. These three compounds (Fig. 7) were reported as non-

torsadogenic by Kramer et al. [5]. When they are categorized according to their TdP risk, nifedipine and diltiazem were categorized as belonging to classes IV or V of the Redfern classification [18], respectively.

The three last compounds (metronidazole, phenytoin and piperacillin) were identified as belonging to profile 7. These compounds (Fig. 4B) induced a gradual TDR decrease associated to an APA decrease (<115 vs. 129 mV in the absence of compounds) and V_{max} decrease (< 128 vs. 245 V/s in the absence of compounds) at 30-fold (phenytoin), 10-fold (metronidazole) or 3-fold (piperacillin) their $EFTPC_{max}$. These compounds (Fig. 6B) showed an I_{Kr} IC_{50} / $EFTPC_{max}$ ratio ranked from 3-fold to 34-fold. As the compounds from profiles 5 and 6, these compounds (Fig. 6B) showed an I_{CaL} IC_{50} lower than their I_{Kr} IC_{50} . They showed, an I_{CaL} vs. I_{Kr} selectivity ranked from 3-fold to 8-fold and an I_{CaL} vs. I_{Na} selectivity ranked from 2-fold to 12-fold. These three compounds (Fig. 7) were reported as non-torsadogenic by Kramer et al. [5].

The present results showed that most of the 32 torsadogenic tested compounds induced a TDR increase while most of the 23 non-torsadogenic tested compounds induced a TDR decrease. Nevertheless, based on their effects on TDR, our study identified seven different profiles of compounds. Is there a relationship between these various compound profiles and their TdP risk according to the Redfern et al. [18] or the CredibleMeds [19] classifications? Even if some exceptions are to be discussed, most of the compounds from Redfern classes I, II and III [18] or from CredibleMeds classes 1, 2 and 3 [19] were identified as inducing a TDR increase. One exception is amiodarone which had no effect on TDR. Nevertheless, this result was not surprising as it was already widely described in literature using various experimental models such as human isolated myocytes or the arterially perfused dog left ventricular wedge preparation [25]. Previous *in silico* studies also demonstrated that amiodarone was ineffective on other proarrhythmia parameter, such as EAD occurrence [4,26]. The classification of sparfloxacin as belonging to class IV of the Redfern classification seemed necessary to be reconsidered as sparfloxacin induced a TDR increase and was categorized as belonging to class 1 of the CredibleMeds classification. The same can be said of risperidone as its classification in Redfern class V [18] is not in agreement with its classification in CredibleMeds

class 2 [19] and its induction of TDR increase, QT increase and TdP [5]. Whether or not it is necessary to give a safety warning signal for dasatinib, donepezil, duloxetine, sitagliptin and telbivudine is yet to be studied in more detail as these compounds induced only a small TDR increase when no torsadogenic risks were reported, except for dasatinib [5]. Metronidazole, phenytoin and piperacillin are probably to be suspected of cardiac liabilities as they induced a TDR decrease associated with the occurrence of an AP with APA and V_{max} decreases which could affect cardiac excitability. This is in accordance with numerous studies reporting the cardiac toxicity of phenytoin, leading to problems such as cardiac arrest [27]. To summarize, the present results showed that the classification of compounds in seven different profiles regarding their effects on TDR was clearly related to the balance not only of their selectivity for I_{Kr} , I_{CaL} or I_{Na} but also their I_{Kr} , I_{CaL} or I_{Na} IC_{50s} / $EFTPC_{max}$ ratio. Most of the tested compounds inducing a TDR increase via I_{Kr} vs. I_{CaL} and/or I_{Na} selective inhibition were torsadogenic and most of the tested compounds inducing a TDR decrease via I_{CaL} vs. I_{Kr} and/or I_{Na} selective inhibition were non-torsadogenic. Based on their profile of activity on TDR, compounds belonging to profile 1 and 7 could probably be excluded from the early research/development process (all class II compounds were identified as belonging to profile 1). A warning could probably put on the compounds belonging to profile 2 and 3 while compounds belonging to profile 4, 5 or 6 could probably appear to be safe. The present results suggest that this methodology could probably also help to determine the classes of compounds not currently categorized with the Redfern or the CredibleMeds TdP risk classifications.

In conclusion, studying the effect of compounds on TDR by *in silico* simulation can probably help to predict their pro-arrhythmic effect. Nevertheless, several limitations for computational prediction of compound pro-arrhythmic activity remain, namely the accuracy of the prerequisite biochemical and/or pharmacological data and the used algorithm. We used the compound data set from Kramer et al. [5] because of they are obtained from human genes. Nevertheless, they were obtained at room temperature (when the used ORd algorithm was tuned for 37°C) and with various computer machines using QPatch and PatchXpress automatic patch system (when it was demonstrated that the best predictive data were obtained from manual patch clamp data despite

their requirement of a high level of expertise and their low throughput [28]). Even if each mathematical algorithm still required refinement in order to reflect the biological reality experimentally observed, we used the ORd algorithm as this algorithm provided the best sensitivity and accuracy for proarrhythmia drug properties prediction [28] (vs. the algorithms of Grandi et al. [29] or ten Tusscher and Panfilov [30] for simulation within the human situation). We used for this study a cycle length of 1000 msec (60 bpm). Since ventricular arrhythmia and EADs can be rate dependent, it would be interesting to conduct further simulations with a range of physiological heart rates such as during sleep (40-50 bpm) or during moderate to vigorous exercise (100 to 150 bpm). As previously described [26], using a higher cycle length for simulation could lead to more sensitive results. Only three ionic currents were taken into account in this work to study the effect of compounds on TDR, but it is certainly useful to consider that many other ionic currents also influence the AP shape and the occurrence of EAD, as already demonstrated by *in silico* simulations [26]. As the effect of I_{Ks} inhibition on the AP is limited under baseline conditions and increased under adrenergic stimulation [31], inclusion of the adrenergic pathway in the stimulation conditions [32] could also be useful in order to fully understand the detailed role of I_{Ks} in TDR. In the same line, the present study was performed only by changing channel conductances. Taking into account current kinetic is certainly also to consider in order to improve safety profile prediction [33]. The present study was restricted to non-failing ventricular myocytes as described in the ORd algorithm. As the failing ventricular tissue is even more at risk for TdP and arrhythmias than the non-failing tissue, it would be also interesting to see under failing ventricle conditions whether certain drugs get their TDR profile re-classified to a less safe profile. Finally, because TdP is a tissue phenomenon, it would be also interesting to done these simulations at a virtual tissue level. The aim of the CiPA initiative [2,3] is precisely to evaluate in more detail the best performance of the various models, and find the best way to produce a dataset to be used in order to obtain the best prediction of cardiac liabilities of compounds.

4. CONCLUSION

Based on computer simulations within the human situation, the present study identified the effects

of various cardiac currents and drugs on TDR amplitude and suggested that *in silico* determination of the effects of drugs on TDR amplitude could be informative for early cardiac safety pharmacology.

CONSENT

It is not applicable.

ETHICAL APPROVAL

It is not applicable.

COMPETING INTERESTS

Author has declared that no competing interests exist.

REFERENCES

1. ICH. Harmonised Tripartite Guideline S7B. Non-clinical evaluation of the potential for delayed ventricular repolarization (QT interval prolongation) by human pharmaceuticals: Step 4 Version; 2005. Available:http://www.ich.org/fileadmin/Public_Web_Site/ICH_Products/Guidelines/Safety/S7B/Step4/S7B_Guideline.pdf (Accessed 5 January 2015).
2. Abernethy D, Brown AM, Colatsky T, Garnett C, Gintant G, January CT, et al. Need for and feasibility of a comprehensive non-clinical safety assay for the pro-arrhythmic potential of new drug; 2013. Available:<http://www.ilsixtra.org/hesi/science/cardiac/cipa/sitePages/Home> (Accessed 10 February 2015).
3. Sager PT, Gintant G, Turner JR, Petit S, Stockbridge N. Rechanneling the cardiac proarrhythmia safety paradigm: A meeting report from the cardiac safety research consortium. *Am Heart J.* 2014;167(3):292-300.
4. Mirams GR, Cui Y, Sher A, Fink M, Cooper J, Heath BM et al. Simulation of multiple ion channel block provides improved early prediction of compounds' clinical torsadogenic risk. *Cardiovasc Res.* 2011; 91(1):53-61.
5. Kramer J, Obejero-Paz CA, Myatt G, Kuryshv YA, Bruening-Wright A, Verducci JS et al. MICE models: Superior to the hERG model in predicting torsade de pointes. *Sci Rep.* 2013;3:2100.

6. Cavero I, Holzgrefe H. Comprehensive in vitro proarrhythmia assay, a novel in vitro/in silico paradigm to detect ventricular proarrhythmic liability: A visionary 21 st century initiative. *Exp Opin Drug Saf.* 2014;13(6):745-58.
7. Kleiman RB, Shah RR, Morganroth JM. Replacing the thorough QT study: Reflections of a baby in the bath water. *Br J Clin Pharmacol.* 2014;78(2):195-201.
8. Moreno JD, Clancy CE. Using computational modeling to predict arrhythmogenesis and antiarrhythmic therapy. *Drug Discov Today Dis Models.* 2009;6(3):71-84.
9. Soubret A, Helmlinger G, Dumortier B, Bibas R, Georgieva A. Modeling and simulation of preclinical cardiac safety: Towards an integrative framework. *Drug Metab Pharmacokinet.* 2009;24(1):76-90.
10. Mirams GR, Noble D. Is it time for in silico simulation of drug cardiac side effects. *Ann N Y Acad Sci.* 2011;1245:44-7.
11. Gintant G. Ions, equations and electrons: The evolving role of computer simulations in cardiac electrophysiology safety evaluations. *Br J Pharmacol.* 2012;167(5): 929-31.
12. Chi KR. Revolution dawning in cardiotoxicity testing. *Nat Rev Drug Discov.* 2013;12(9):565-7.
13. Said TH, Wilson LD, Jeyaraj D, Fossa AA, Rosenbaum DS. Transmural dispersion of repolarization as a preclinical marker of drug-induced proarrhythmia. *J Cardiovasc Pharmacol.* 2012;60(2):165-71.
14. O'Hara T, Virág L, Varró A, Rudy Y. Simulation of the undiseased human cardiac ventricular action potential: Model formulation and experimental validation. *PLoS Comput Biol.* 2011;7(5):e1002061.
15. Glukhov AV, Fedorov VV, Lou Q, Ravikumar VK, Kalish PW, Schuessler RB et al. Transmural dispersion of repolarization in failing and nonfailing human ventricle. *Circ Res.* 2010;106(5): 981-91.
16. Antzelevitch C, Sicouri S, Litovsky SH, Lukas A, Krishnan SC, Di Diego JM, et al. Heterogeneity within the ventricular wall: Electrophysiology and pharmacology of epicardial, endocardial, and M cells. *Circ Res.* 1991;69(6):1427-49.
17. Yan GX, Antzelevitch C. Cellular basis for the normal T wave and the electrocardiographic manifestations of the long-QT syndrome. *Circulation.* 1998; 98(18):1928-36.
18. Redfern WS, Carlsson L, Davis AS, Lynch WG, MacKenzie I, Palethorpe S et al. Relationships between preclinical cardiac electrophysiology, clinical QT interval prolongation and torsade de pointes for a broad range of drugs: Evidence for a provisional safety margin in drug development. *Cardiovasc Res.* 2003;58(1): 32-45.
19. Woosley RL. CredibleMeds® list of QT prolonging medications. Available: <http://www.CredibleMeds.org> (Accessed 29 January 2015).
20. Lawrence CL, Pollard CE, Hammond TG, Valentin JP. Nonclinical proarrhythmia models: Predicting Torsades de Pointes. *J Pharmacol Toxicol Methods.* 2005;52(1): 46-59.
21. Antzelevitch C. Ionic, molecular, and cellular bases of QT-interval prolongation and torsade de pointes. *Europace.* 2007; 9(Suppl 4):4,4-15.
22. Antzelevitch C. Drug-induced spatial dispersion of repolarisation. *Cardiol J.* 2008;15(2):100-21.
23. Shimizu W, Antzelevitch C. Sodium channel block with mexiletine is effective in reducing dispersion of repolarisation and preventing torsade de pointes in LQT2 and LQT3 models of long QT syndrome. *Circulation.* 1997;96(6):2038-47.
24. Sicouri S, Glass A, Ferreiro M, Antzelevitch C. Transseptal dispersion of repolarization and its role in the development of Torsade de Pointes arrhythmias. *J Cardiovasc Electrophysiol.* 2010;21(4):441-7.
25. Merot J, Charpentier F, Poirier JM, Coutris G, Weissenburger J. Effects of chronic treatment by amiodarone on transmural heterogeneity of canine ventricular repolarization in vivo: Interactions with acute sotalol. *Cardiovasc Res.* 1999;44(2): 303-14.
26. Christophe B. Simulation of early after-depolarisation in non failing human ventricular myocytes: Can this help cardiac safety pharmacology? *Pharmacol Rep.* 2013;65(5):1281-93.
27. York RC, Coleridge ST. Cardiopulmonary arrest following intravenous phenytoin loading. *Am J Emerg Med.* 1988;6(3):255-9.
28. Mirams GR, Davies MR, Brough SJ, Bridgland-Taylor MH, Cui Y, Gavaghan DJ

- et al. Prediction of Thorough QT study results using action potential simulations based on ion channel screens. *J Pharmacol Toxicol Methods*. 2014;70(3): 246-54.
29. Grandi E, Pasqualini FS, Bers DM. A novel computational model for the human ventricular action potential and Ca transient. *J Mol Cell Cardiol*. 2010;48(1): 112-121.
30. ten Tusscher KH, Panfilov AV. Cell model for efficient simulation of wave propagation in human ventricular tissue under normal and pathological conditions. *Phys Med Biol*. 2006;51(23):6141-56
31. Jost N, Virag L, Bitay M, Tacacks J, Lengyel C Biliczki P, et al. Restricting excessive cardiac action potential and QT prolongation: A vital role for IKs in human ventricular muscle. *Circulation*. 2005; 112(10):1392-9
32. O'Hara T, Rudy Y. Quantitative comparison of cardiac ventricular myocyte electrophysiology and response to drugs in human and nonhuman species. *Am J Physiol Heart Circ Physiol*. 2011; 302(5):H1023-30.
33. Di Veroli GY, Davies MR, Zhang H, Abi-Gerges N, Boyett MR. High throughput screening of drug binding dynamics to hERG improves early drug safety assessment. *Am J Physiol Heart Circ Physiol*. 2013;304(1):H104-H17.

© 2015 Christophe; This is an Open Access article distributed under the terms of the Creative Commons Attribution License (<http://creativecommons.org/licenses/by/4.0>), which permits unrestricted use, distribution, and reproduction in any medium, provided the original work is properly cited.

Peer-review history:

The peer review history for this paper can be accessed here:
<http://www.sciencedomain.org/review-history.php?iid=1177&id=14&aid=9467>